Viscoelastic Analysis of Laminated Plate Buckling

Dale W. Wilson* and Jack R. Vinson†
University of Delaware, Newark, Delaware

Linear viscoelasticity theory was used in the formulation of a general buckling theory for fiber-reinforced composite laminated plates. The theory includes the effects of transverse shear and normal deformation (TSD and TND, respectively) and bending-extensional coupling of time-dependent buckling response. Anisotropic viscoelastic constants were determined using the Tsai-Halpin equations, assuming elastic fiber properties in combination with a power law viscoelastic model for the matrix properties. The governing equations of plate buckling were developed using the Theorem of Minimum Potential Energy, and the Rayleigh-Ritz method was employed in the solution of the governing equations for specific boundary conditions. Results are presented comparing viscoelastic solutions based on classical analysis, analysis including TSD effects, and analysis including both TSD and TND effects for simply supported plate subjected to inplane compressive loading ($N_{xy}=0$).

Nomenclature

a = plate dimension in x direction
a_T = temperature shift parameter
a_H = moisture shift parameter
$A_{ij}(t)$ = viscoelastic extensional stiffnesses
b = plate dimension in y direction
$B_{ij}(t)$ = viscoelastic bending-extensional coupling stiffnesses
$D_{ij}(t)$ = viscoelastic bending stiffnesses
$E_m(t)$ = viscoelastic Young's modulus of the matrix
E_f = Young's modulus of the fiber
F_i = body forces
$G_m(t)$ = viscoelastic shear modulus of the matrix
K_m = bulk modulus of the matrix
M = weight percent of moisture
N_x, N_y = total inplane force resultant in x and y directions, respectively
N_{xy} = total inplane shear force resultant
$\bar{Q}_{ijkl}(t)$ = viscoelastic stiffness terms transformed to the plate coordinate system
$S_{ijkl}(t)$ = viscoelastic creep compliances
T = temperature
T_i = surface tractions
t = time
τ = reduced time
u, v, w = displacements in x, y, and z directions, respectively
u^0 = laminate midplane displacements in y direction
v^0 = laminate midplane displacements in y direction
V_f = volume fraction of fibers in composite
$W(t)$ = viscoelastic strain energy
γ = creep compliance power law exponent
α_{ij} = coefficients of thermal expansion
β_{ij} = coefficients of moisture expansion
λ = ratio of loading in y direction to loading in x direction, N_y/N_x

Introduction

WITH the upsurge of interest by the aerospace industry in using advanced composites for primary load-bearing structures, accurate design and analysis methods are becoming more critical. Most design and analysis techniques for composites assume anisotropic elastic behavior,[1] and for cases where most of the load is carried by the fibers, the assumption is satisfactory. However, properties transverse to the fibers and shear properties are matrix controlled and exhibit strong viscoelastic behavior.[2,3] There are many cases where the transverse and shear stiffnesses significantly affect the material response, and time-dependent behavior must be examined.

The buckling response of laminated plates is one case where transverse normal and shear response has been shown to be significant for certain geometries, loading conditions, and boundary conditions.[4-8] While the viscoelastic buckling response of laminated plates has been examined,[9] classical theory was used which largely ignores bending-extensional coupling, transverse shear deformation (TSD), and transverse normal deformation (TND) effects, three responses controlled by strongly viscoelastic properties.

Results of an investigation to assess the significance of viscoelastic effects on the buckling response of laminated plates are reported in this paper. A general viscoelastic buckling analysis was formulated using the simplifying assumption of linear viscoelasticity employing the quasielastic approximation. The analysis included bending-extensional coupling and transverse shear and normal deformations. Case studies for a simply supported plate subjected to inplane compressive loading were used to investigate the effects of plate geometry, loading configuration, and laminate configuration on viscoelastic buckling response.

Viscoelastic Considerations

The viscoelastic properties of continuous fiber-reinforced plastic composite systems are orthotropic. While the response of the material ranges from nearly elastic in the fiber direction to nonlinear viscoelastic in shear, linear viscoelastic response is assumed in the current investigation. Research reported in the literature[2,9] indicates that this assumption is reasonable for glass/epoxy and graphite/epoxy composites.

The constitutive relation for a linear viscoelastic anisotropic material is:

$$E_{ij}(t) = \int_{-\infty}^{t} S_{ijkl}(t-t') \frac{d\sigma_{kl}(t)}{dt'} dt' \qquad (1)$$

Formulation of the viscoelastic governing equation for plate buckling is based on these relations. Sims[9] showed that for cases where the applied load is nearly timewise constant, the

Received March 22, 1983; revision received Aug. 22, 1983.

*Associate Scientist, Center for Composite Materials.
†H. Fletcher Brown Professor, Department of Mechanical and Aerospace Engineering. Associate Fellow AIAA.

Table 1 Material properties assumed for a graphite/epoxy composite

Fiber modulus, longitudinal (E_{fl})	165.5 GPa	24.0×10^6 psi
Fiber modulus, transverse (E_{ft})	13.8 GPa	2.0×10^6 psi
Fiber Poisson's ratio (ν_{LT})		0.3
Fiber shear modulus (G_{LT})	27.5 GPa	4.0×10^6 psi
Matrix modulus, initial (E_{m_0})	4.6 GPa	0.67×10^6 psi
Matrix Poisson's ratio (ν_{m_0})		0.3
Constants for power law compliance formulation		
$S_{11}=b't^{\gamma}$ (b')	2.0×10^{-2} Pa^{-1}	0.291×10^{-5} psi^{-1}
(γ)		0.20
Fiber volume fraction (V_f)		0.62

correspondence principle results reduce approximately to those obtained by direct substitution of time-varying properties into the elastic formulation of the problem. The error incurred by making this quasielastic approximation is less than 10% for a typical graphite/epoxy composite, and results in considerable simplification by negating the need to perform inverse Laplace transformation of the associated elastic problem.‡ This error was deemed satisfactory in light of the analytical simplifications achieved, since the study is a comparative one investigating the significance of including transverse shear deformation (TSD) and transverse normal deformation (TND) effects on the viscoelastic buckling behavior of plates.

Viscoelastic Property Determination

Since the quasielastic method of solution has been employed, the viscoelastic effects are expressed in the buckling analysis solely by the creep compliances or relaxation moduli. A survey of the literature quickly reveals that a complete set of viscoelastic data for graphite/epoxy (or any other system) is not available. Viscoelastic data were available for epoxy resin, and therefore, a micromechanical materials modeling approach was used to determine the necessary properties.

The Tsai-Halpin equations have been used, assuming that orthotropic elastic fibers are embedded in a viscoelastic, isotropic matrix. The properties assumed for graphite fibers are given in Table 1, with all other important material property data. A power law formulation is assumed for the matrix creep compliance,[9] as shown below:

$$S_m(t)=b't^{\gamma} \tag{2}$$

where values for b' and γ are given in Table 1. The Young's modulus is a more convenient form, so this expression is inverted using the correspondence principle to give

$$E_m(t)=\frac{1}{\Gamma(1+\gamma)\Gamma(1-\gamma)S_m(t)} \tag{3}$$

which is the exact inversion of Eq. (2) accomplished using LT theory, where $\Gamma(\alpha)$ is the gamma function. This was done to minimize error in $E_m(t)$ which could subsequently propagate into the relaxation moduli of the components.

Two other matrix properties are necessary to characterize its viscoelastic response completely: $\nu_m(t)$ and $G_m(t)$, the

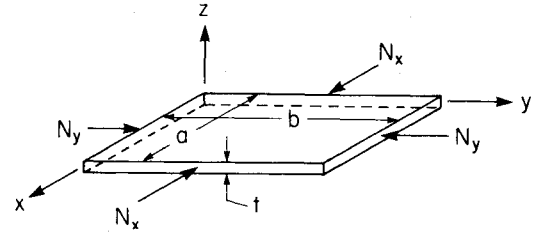

Fig. 1 Plate geometry and loading conditions.

Poisson's ratio and shear modulus, respectively. The Poisson's ratio is found by assuming the bulk modulus to be a constant and determined from

$$K_m=E_m(0)/3[1-2\nu_m(0)] \tag{4}$$

Knowing K_m, the Poisson's ratio is found to be

$$\nu_m(t)=\tfrac{1}{2}(1-E_m(t)/3K_m) \tag{5}$$

and the shear modulus is found to be

$$G_m(t)-E_m(t)/2[1+\nu_m(t)] \tag{6}$$

Using the Tsai-Halpin relations,[11] the effective viscoelastic properties of the composite $E_1(t)$, $E_2(t)$, $E_3(t)$, $\nu_{12}(t)$, $\nu_{13}(t)$, $\nu_{23}(t)$, $G_{12}(t)$, $G_{13}(t)$, and $G_{23}(t)$ are determined. Again the property information is given in Table 1. Effectively, the longitudinal properties (E_1,ν_{12},ν_{13}) conform to the rule of mixtures:

$$P_1(t)=P_fV_f+P_m(t)[1-V_f] \tag{7}$$

The transverse and shear properties (E_2,E_3,G_{12},G_{23}, etc.) are approximated by

$$P(t)=P_m(t)\left[\frac{P_f(1-\xi_iV_f)+\xi_iP_m(t)(1-V_f)}{P_f(1-V_f)+P_m(t)(\xi_i+V_f)}\right] \tag{8}$$

where ξ_i is an empirical parameter related to the packing geometry, and P_f§ and P_m refer to the fiber and matrix properties (ξ_i is 1 for the packing geometry assumed).

These basic viscoelastic lamina properties are substituted for their elastic equivalents in laminated plate theory under

‡The associated elastic problem is the term applied to the elastic formulation of a viscoelastic problem in the Laplace transform (LT) domain allowed by the correspondence principle.

§Note that P_f is timewise constant, in accordance with the earlier assumption of elastic behavior.

the quasielastic assumption. Laminated plate theory is then used exactly as in elastic analysis.

Derivation of the Buckling Equation

A simply supported plate whose geometry and loading conditions are described in Fig. 1 was used in the case studies. Small deflection theory was assumed, but transverse shear and transverse normal deformation were included. Given these assumptions, the strain displacement relations used were

$$\epsilon_x(t)=\frac{\partial u(t)}{\partial x} \qquad \gamma_{yz}(t)=\frac{\partial v(t)}{\partial z}+\frac{\partial w(t)}{\partial y}$$

$$\epsilon_y(t)=\frac{\partial v(t)}{\partial y} \qquad \gamma_{xz}(t)=\frac{\partial u(t)}{\partial z}+\frac{\partial w(t)}{\partial x}$$

$$\epsilon_z(t)=\frac{\partial w(t)}{\partial z} \qquad \gamma_{xy}(t)=\frac{\partial u(t)}{\partial y}+\frac{\partial v(t)}{\partial x} \tag{9}$$

The displacement fields in the strain displacement relations were of the form

$$u(x,y,z,t)=u^0(x,y,t)+zF_x(x,y,t)$$

$$v(w,y,z,t)=v^0(x,y,t)+zF_y(x,y,t)$$

$$w(x,y,z,t)=w^0(x,y,t)+f_1F_z(z) \tag{10}$$

where f_1 is a tracing constant employed to include TND effects ($f_1=1$). Substituting Eq. (10) into Eq. (9), the strain displacement relations become

$$\epsilon_x(t)=\frac{\partial u^0(t)}{\partial x}+Z\frac{\partial F_x(t)}{\partial x}$$

$$\epsilon_y(t)=\frac{\partial v^0(t)}{\partial y}+Z\frac{\partial F_y(t)}{\partial y}$$

$$\epsilon_z(t)=f_1\frac{\partial F_z(t)}{\partial z}$$

$$\gamma_{xz}=F_x(t)+\frac{\partial w^0(t)}{\partial x}$$

$$\gamma_{yz}=F_y(t)+\frac{\partial w^0(t)}{\partial y}$$

$$\gamma_{xy}=\left[\frac{\partial u^0(t)}{\partial y}+\frac{\partial v^0(t)}{\partial x}\right]+Z\left[\frac{\partial F_x(t)}{\partial y}+\frac{\partial F_y(t)}{\partial x}\right] \tag{11}$$

Using tensor notation, the constitutive relation for the kth viscoelastic lamina (assuming the quasielastic approximation) in a laminated plate, transformed to the plate coordinate system is

$$\sigma_i^k(t)=\bar{Q}_{ij}^k(t)\cdot\epsilon_i^k(t) \qquad i,j=1,2,\ldots,6 \tag{12}$$

where in the contracted notation, $\sigma_{ii}=\sigma_i$ for $i=1,2,3$, $\sigma_{23}=\sigma_4$, $\sigma_{13}=\sigma_5$, and $\sigma_{12}=\sigma_6$.

The theorem of minimum potential energy was used to derive the governing equation of buckling. The total potential energy for a viscoelastic solid, assuming the quasielastic approach is

$$V(t)=\int_R W(t)\,\mathrm{d}R-\int_S T_i(t)u_i(t)\,\mathrm{d}S-\int_R F_iu_i(t)\,\mathrm{d}R \tag{13}$$

The body forces are negligible, and for buckling, the only surface tractions considered were the inplane force resultants $N_x(t)$, $N_y(t)$, and $N_{xy}(t)$. Expanding Eq. (13), the total potential energy is expressed

$$V=\frac{1}{2}\sum_{k=1}^{n}\iint_A\int_{h_k}^{h_{k+1}}\{\epsilon_x\sigma_x+\epsilon_y\sigma_y+\epsilon_z\sigma_z+\epsilon_{yz}\sigma_{yz}+\epsilon_{xz}\sigma_{xz}+\epsilon_{xy}\sigma_{xy}\}^k\,\mathrm{d}A-\iint_A\left\{N_x\left[\frac{\partial u^0}{\partial x}+\frac{1}{2}\left(\frac{\partial w^0}{\partial x}\right)^2\right]+N_{xy}\left[\frac{\partial u^0}{\partial y}+\frac{\partial v^0}{\partial x}+\frac{\partial^2 w^0}{\partial x\partial y}\right]+N_y\left[\frac{\partial v^0}{\partial y}+\frac{1}{2}\left(\frac{\partial w^0}{\partial y}\right)^2\right]\right\}\mathrm{d}A \tag{14}$$

Following the usual procedures of substituting the constitutive equations and strain-displacement relations into Eq. (14), the total potential energy was found in terms of viscoelastic stiffnesses, plate displacements, and applied loads. The equation for the total potential energy with all terms not containing $F_z(t)$ integrated through the plate thickness is given next.

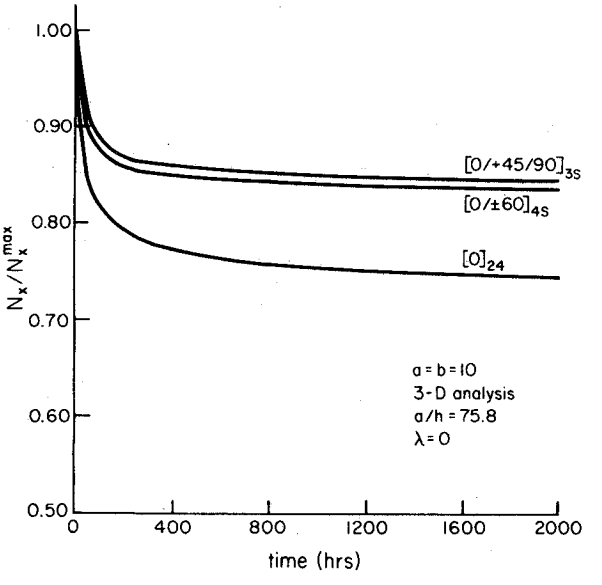

Fig. 2 Buckling response as a function of laminate configuration.

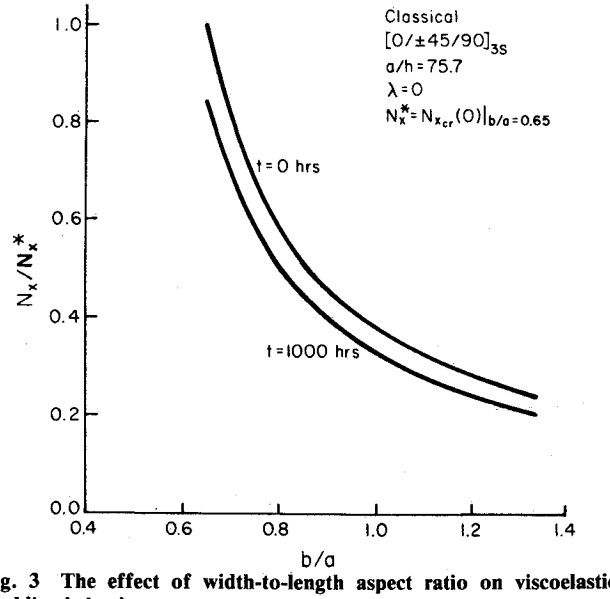

Fig. 3 The effect of width-to-length aspect ratio on viscoelastic buckling behavior.

$$V=\frac{1}{2}\iint_A \Big\{A_{11}(t)\Big(\frac{\partial u^0(t)}{\partial x}\Big)^2+2A_{12}(t)\frac{\partial u^0(t)}{\partial x}\frac{\partial v^0(t)}{\partial y}+2A_{16}(t)\Big(\frac{\partial^2 u^0(t)}{\partial x\partial y}+\frac{\partial u^0(t)}{\partial x}\frac{\partial v^0(t)}{\partial x}\Big)+A_{22}(t)\Big(\frac{\partial v^0(t)}{\partial y}\Big)^2$$
$$+2A_{26}(t)\Big(\frac{\partial v^0(t)}{\partial y}\frac{\partial u^0(t)}{\partial y}+\frac{\partial^2 v^0(t)}{\partial x\partial y}\Big)+A_{44}(t)\Big[F_y^2(t)+2F_y(t)\frac{\partial w^0(t)}{\partial y}+\Big(\frac{\partial w^0(t)}{\partial y}\Big)^2\Big]$$
$$+2A_{45}\Big[F_x(t)F_y(t)+F_y(t)\frac{\partial w^0(t)}{\partial x}+F_x(t)\frac{\partial w^0(t)}{\partial y}+\frac{\partial^2 w^0(t)}{\partial x\partial y}\Big]+A_{55}\Big[F_x^2(t)+2F_x\frac{\partial w^0(t)}{\partial x}+\Big(\frac{\partial w^0(t)}{\partial x}\Big)^2\Big]$$
$$+A_{66}(t)\Big[\Big(\frac{\partial u^0(t)}{\partial y}\Big)^2+\frac{\partial u^0(t)}{\partial y}\frac{\partial v^0(t)}{\partial x}+\Big(\frac{\partial v^0(t)}{\partial x}\Big)^2\Big]+2B_{11}(t)\Big(\frac{\partial u^0(t)}{\partial x}\frac{\partial F_x(t)}{\partial x}\Big)+2B_{22}(t)\Big(\frac{\partial v^0(t)}{\partial y}\frac{\partial F_y(t)}{\partial y}\Big)$$
$$+2B_{16}(t)\Big(\frac{\partial u^0(t)}{\partial x}\frac{\partial F_x(t)}{\partial y}+\frac{\partial u^0(t)}{\partial x}\frac{\partial F_y(t)}{\partial x}+\frac{\partial u^0(t)}{\partial y}\frac{\partial F_x(t)}{\partial x}+\frac{\partial v^0(t)}{\partial x}\frac{\partial F_x(t)}{\partial x}\Big)+2B_{12}\Big(\frac{\partial u^0(t)}{\partial x}\frac{\partial F_y(t)}{\partial y}+\frac{\partial v^0(t)}{\partial y}\frac{\partial F_x(t)}{\partial x}\Big)$$
$$+B_{26}\Big(\frac{\partial v^0(t)}{\partial y}\frac{\partial F_x(t)}{\partial y}+\frac{\partial v^0(t)}{\partial y}\frac{\partial F_y(t)}{\partial x}+\frac{\partial u^0(t)}{\partial y}\frac{\partial F_y(t)}{\partial y}+\frac{\partial v^0(t)}{\partial x}\frac{\partial F_y(t)}{\partial y}\Big)+2B_{66}(t)\Big(\frac{\partial u^0(t)}{\partial y}\frac{\partial F_x(t)}{\partial y}+\frac{\partial u^0(t)}{\partial y}\frac{\partial F_y(t)}{\partial x}$$
$$+\frac{\partial v^0(t)}{\partial x}\frac{\partial F_x(t)}{\partial y}+\frac{\partial v^0(t)}{\partial x}\frac{\partial F_y(t)}{\partial x}\Big)+D_{11}(t)\Big(\frac{\partial F_x(t)}{\partial x}\Big)^2+2D_{12}(t)\Big(\frac{\partial F_x(t)}{\partial x}\frac{\partial F_y(t)}{\partial y}\Big)$$
$$+2D_{16}(t)\Big(\frac{\partial F_x(t)}{\partial x}\frac{\partial F_x(t)}{\partial y}+\frac{\partial F_x(t)}{\partial x}\frac{\partial F_y(t)}{\partial x}\Big)+D_{22}(t)\Big(\frac{\partial F_y(t)}{\partial y}\Big)^2+2D_{26}(t)\Big(\frac{\partial F_y(t)}{\partial y}\frac{\partial F_x(t)}{\partial y}+\frac{\partial F_y(t)}{\partial y}\frac{\partial F_y(t)}{\partial x}\Big)$$
$$+D_{66}(t)\Big[\Big(\frac{\partial F_x(t)}{\partial y}\Big)^2+2\frac{\partial F_x(t)}{\partial y}\frac{\partial F_y(t)}{\partial x}+\Big(\frac{\partial F_y(t)}{\partial x}\Big)^2\Big]+\frac{1}{2}\sum_{k=1}^{n}\iint_A\int_{h_k}^{h_{k+1}} f_l\Big[2\frac{\partial u^0(t)}{\partial x}\bar{Q}_{13}^k(t)\frac{\partial F_z(t)}{\partial z}$$
$$+2\frac{\partial F_x(t)}{\partial x}\bar{Q}_{13}^k(t)z\frac{\partial F_z(t)}{\partial z}+2\frac{\partial v^0}{\partial y}\bar{Q}_{23}^k(t)\frac{\partial F_z(t)}{\partial z}+2\frac{\partial F_y(t)}{\partial y}\bar{Q}_{23}^k(t)z\frac{\partial F_z(t)}{\partial z}+\bar{Q}_{33}^k(t)\Big(\frac{\partial F_z(t)}{\partial z}\Big)^2$$
$$+2\Big(\frac{\partial u^0(t)}{\partial y}+\frac{\partial v^0(t)}{\partial x}\Big)\bar{Q}_{36}^k(t)\frac{\partial F_z(t)}{\partial z}+2\Big(\frac{\partial F_x(t)}{\partial y}+\frac{\partial F_y(t)}{\partial x}\Big)\bar{Q}_{36}^k z\frac{\partial F_z(t)}{\partial z}\Big]\mathrm{d}z\mathrm{d}A$$
$$-\iint_A\Big\{N_x(t)\Big[\frac{\partial u^0(t)}{\partial x}+\frac{1}{2}\Big(\frac{\partial w^0(t)}{\partial x}\Big)^2\Big]+N_{xy}(t)\Big[\frac{\partial u^0(t)}{\partial y}+\frac{\partial v^0(t)}{\partial x}+\frac{\partial^2 w^0(t)}{\partial x\partial y}\Big]+N_y(t)\Big[\frac{\partial v^0(t)}{\partial y}+\frac{1}{2}\Big(\frac{\partial w^0(t)}{\partial y}\Big)^2\Big]\Big\}\mathrm{d}A \tag{15}$$

where f_l is a tracing constant to determine effects of transverse normal strain (note $\sigma_z=0$ was assumed), and

$$A_{ij}(t)=\sum_{k=1}^{n}\bar{C}_{ij}^k(h_{k+1}-h_k)$$
$$B_{ij}(t)=\frac{1}{2}\sum_{k=1}^{n}\bar{C}_{ij}^k(h_{k+1}^2-h_k^2)$$
$$D_{ij}(t)=\frac{1}{3}\sum_{k=1}^{n}\bar{C}_{ij}^k(h_{k+1}^3-h_k^3)$$

Buckling occurs when the total potential energy is a minimum at a stationary point (the first variation is zero), and the second variation exists and is positive definite. Taking the variation of the total potential energy results in a set of Euler-Lagrange equations and associated natural boundary conditions. Mathematically this is stated

$$\delta V(t)=\iint_A[\,(\,)\delta u^0(t)+(\,)\delta v^0(t)+(\,)\delta w^0(t)+(\,)\delta F_x(t)+(\,)\delta F_y(t)\,]\mathrm{d}A+\sum_{k=1}^{n}\iint_{h_k}^{h_{k+1}}(\,)\delta F_z(t)\mathrm{d}z\mathrm{d}A$$
$$+\text{natural boundary conditions} \tag{16}$$

where ( ) represents equations. In order to satisfy the conditions that $\delta V(t)=0$, each bracketed equation must be zero.

The Euler-Lagrange equations were used to determine approximate expressions for $F_x(x,y,t)$, $F_y(x,y,t)$, and $F_z(z,t)$ as a function of the midplane deflection, w^0. This was accomplished for $F_x(x,y,t)$ and $F_y(x,y,t)$ by reducing the Euler-Lagrange equations to the form of beam equations in the x and y directions. For $F_x(x,t)$, the Euler-Lagrange equations are

$$A_{11}(t)\frac{\mathrm{d}^2u^0(t)}{\mathrm{d}x^2}+B_{11}(t)\frac{\mathrm{d}^2F_x(t)}{\mathrm{d}x^2}=0$$
$$A_{55}(t)\frac{\mathrm{d}F_x(t)}{\mathrm{d}x}+A_{55}(t)\frac{\mathrm{d}^2w^0(t)}{\mathrm{d}x^2}-\bar{N}_x(t)\frac{\mathrm{d}^2w^0(t)}{\mathrm{d}x^2}=0$$
$$-A_{55}(t)F_x(t)-A_{55}(t)\frac{\mathrm{d}w^0(t)}{\mathrm{d}x}+B_{11}(t)\frac{\mathrm{d}^2u^0(t)}{\mathrm{d}x^2}$$
$$+D_{11}(t)\frac{\mathrm{d}^2F_x(t)}{\mathrm{d}x^2}=0 \tag{17}$$

Solving for $F_x(x,t)$

$$F_x(x,t)=-\frac{\mathrm{d}w^0(t)}{\mathrm{d}x}-\Big(\frac{D_{11}(t)A_{11}(t)-B_{11}^2(t)}{A_{11}(t)}\Big)\times\Big(\frac{A_{55}(t)-N_x(t)}{A_{55}^2(t)}\Big)\frac{\mathrm{d}^3w^0(t)}{\mathrm{d}x^3} \tag{18}$$

Generalizing to a plate by adding y dependence

$$F_x(x,y,t)=-\frac{\partial w^0(t)}{\partial x}-\Big(\frac{D_{11}(t)A_{11}(t)-B_{11}^2(t)}{A_{11}(t)}\Big)\times\Big(\frac{A_{55}(t)-\bar{N}_x}{A_{55}^2(t)}\Big)\frac{\partial^3w^0(t)}{\partial x^3} \tag{19}$$

The expression for $F_y(x,y,t)$ is found similarly using the appropriate Euler-Lagrange equations.

An approximation for the function $\partial F_z(t)/\partial z$ was found by integrating the Euler-Lagrange equation associated with ∂F_z with respect to z. The Euler-Lagrange equation is

$$f_1\left[\bar{Q}^k_{13}\frac{\partial F_x(t)}{\partial x}+\bar{Q}^k_{23}\frac{\partial F_y(t)}{\partial y}+\bar{Q}^k_{36}\left(\frac{\partial F_x(t)}{\partial y}+\frac{\partial F_y(t)}{\partial x}\right)+\bar{Q}^k_{33}\frac{\partial^2 F_z(t)}{\partial z^2}\right]=0 \tag{20}$$

Integrating

$$\frac{\partial F_z(t)}{\partial z}=\frac{f_1}{\bar{Q}^k_{33}}\left[-\bar{Q}^k_{13}\frac{\partial F_x(t)}{\partial x}-\bar{Q}^k_{23}\frac{\partial F_y(t)}{\partial y}-\bar{Q}^k_{36}\left(\frac{\partial F_x(t)}{\partial y}+\frac{\partial F_y(t)}{\partial x}\right)\right]+C \tag{21}$$

Substituting into the natural boundary condition, the constant C is found to be

$$C=\frac{1}{\bar{Q}^k_{33}}\left[-\bar{Q}^k_{13}\frac{\partial u^0(t)}{\partial x}-\bar{Q}^k_{23}\frac{\partial v^0(t)}{\partial y}-\bar{Q}^k_{36}\left(\frac{\partial u^0}{\partial y}+\frac{\partial v^0}{\partial x}\right)\right]$$

With the mathematical form of $F_z(t)$ defined, it can be substituted into the total potential energy, Eq. (15), and the volume integral reduced to an area integral by integrating across the plate stiffness.

The Rayleigh-Ritz method is used to solve the governing equation. For the simply supported plate, the assumed displacement functions are chosen to satisfy the following boundary conditions:

$$w^0=0, \qquad M_n=0, \qquad N_{nt}=0, \qquad u^0_n=0$$

where n and t refer to the normal and tangential direction with respect to the boundary. The displacement functions are selected to satisfy the geometric boundary conditions, and are of the following double series form

$$u^0(x,y,t)=\sum_{m=1}^{\infty}\sum_{n=1}^{\infty}A_{mn}(t)\sin\frac{m\pi x}{a}\cos\frac{n\pi y}{b}$$

$$v^0(x,y,t)=\sum_{m=1}^{\infty}\sum_{n=1}^{\infty}B_{mn}(t)\cos\frac{m\pi x}{a}\sin\frac{n\pi y}{b}$$

$$w^0(x,y,t)=\sum_{m=1}^{\infty}\sum_{n=1}^{\infty}C_{mn}(t)\sin\frac{m\pi x}{a}\sin\frac{n\pi y}{b} \tag{22}$$

Substitution of these assumed displacement functions back into the governing equation and taking the variation with respect to the unknown displacement amplitudes A_{mn}, B_{mn}, and C_{mn} sets forth the eigenvalue problem

$$\begin{bmatrix}E_{11}&E_{12}&E_{13}\\E_{21}&E_{22}&E_{23}\\E_{31}&E_{32}&E_{33}\end{bmatrix}\begin{Bmatrix}A_{mn}\\B_{mn}\\C_{mn}\end{Bmatrix}=N_x\begin{bmatrix}0&0&F_{13}\\0&0&F_{23}\\F_{31}&F_{32}&F_{33}\end{bmatrix}\times\begin{Bmatrix}A_{mn}\\B_{mn}\\C_{mn}\end{Bmatrix}+N_x^2\begin{bmatrix}0&0&0\\0&0&0\\0&0&G_{33}\end{bmatrix}\begin{Bmatrix}A_{mn}\\B_{mn}\\C_{mn}\end{Bmatrix} \tag{23}$$

where $N_{xy}=0$ and $N_y=\lambda N_x$. Each E_{ij}, F_{ij}, and G_{ij} term above is an algebraic sum of the products of laminate stiffnesses and mode shape parameters of the form $m\pi/a$ or $n\pi/b$ for the x and y directions, respectively. They are the coefficients of the displacement amplitudes resulting from taking the first variation of the total potential energy with respect to each of the unknown displacement amplitudes.

Notice that for the Rayleigh-Ritz method to give approximate solutions to the governing equation, the assumed form of the displacement functions need only satisfy the geometric boundary conditions. For the cases where $D_{16}(t)$ and $D_{26}(t)$ do not vanish, the natural boundary conditions are not satisfied. In this case convergence of the approximate solution to the exact solution is slow.

Using a Gauss-Jordan reduction, Eq. (23) can be simplified to give

$$[E(t)]\{C_{mn}(t)\}=N_x(t)[F(t)]\{C_{mn}(t)\}+N_x^2(t)[G(t)]\{C_{mn}(t)\} \tag{24}$$

which is a function of the single unknown displacement amplitude, C_{mn}. Here the terms $E(t)$, $F(t)$, and $G(t)$ are the sums of the known E_{ij}, F_{ij}, and G_{ij} terms resulting from the above algebraic manipulation. The definitions of these terms are identical to those defined by Flaggs.[8]

The critical buckling load is determined by finding the minimum eigenvalue from the solution of Eq. (24). Since the eigenvalue problem contains quadratic terms, the solution must be found by an iterative approach. This can be accomplished by first solving the uncoupled problem

$$[E(t)]\{C_{mn}(t)\}=N_x(t)[F(t)]\{C_{mn}(t)\} \tag{25}$$

the solution of which is used as a first approximation in the iterative solution of the whole problem. Numerical methods have been employed in the actual solution of the eigenvalue problem.

Verification of the Analysis

In order to verify the analysis, a test case was studied using $[0/\pm45/90]_s$ and $[0/\pm60]_s$ laminates. The material property data set used in the determination of the viscoelastic properties was shown previously in Table 1. The plate dimensions are $a=b=25.4$ cm (10.0 in.), and there is no inplane loading in the y direction. The plate is assumed to be at a uniform temperature of 297 K (75°F). Verification consists of comparing the classical solution of the problem

Table 2 Comparison of results for simply supported plate buckling, $a/h=227$, N/m (lb_f/in.)

Laminate	Classical	Uncoupled	TSD	3-D
$[0/\pm45/90]_s$	3176 (18.14)	3176 (18.14)	3176 (18.14)	3176 (18.15)
$[0/\pm60]_s$	1220 (6.97)	1220 (6.97)	1220 (6.97)	1220 (6.98)

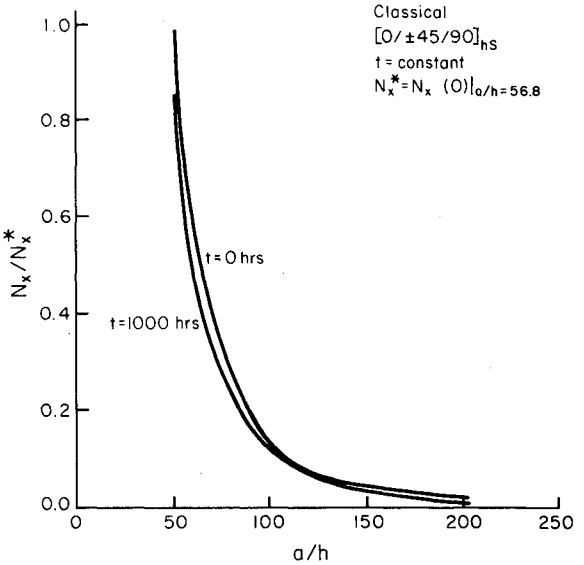

Fig. 4 The effect of plate thickness-to-length aspect ratio on viscoelastic buckling response.

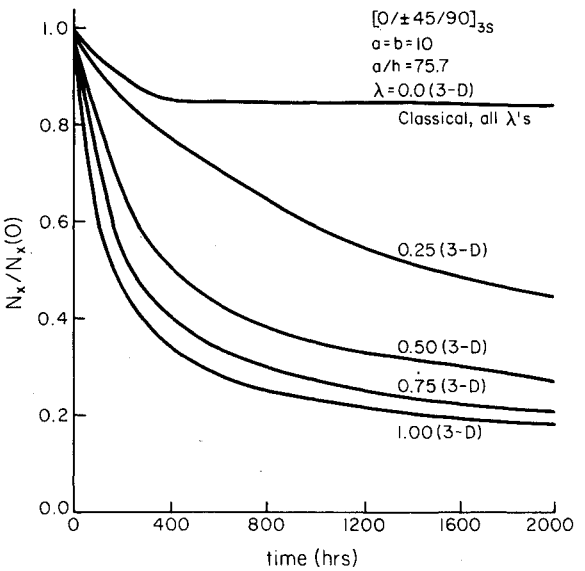

Fig. 5 The effect of load ratio on viscoelastic buckling behavior.

found previously[1] to the present solutions, including the uncoupled solution and solutions incorporating transverse shear deformation (TSD) and combined TSD and transverse normal deformations (3-D). The results show very close agreement at zero time, as given in Table 2.

These test cases represent special conditions wherein the laminate is balanced and symmetric about the midplane, and is of a geometry which minimizes TSD and TND effects by having the ratio inplane plate dimensions to thickness greater than 100.

Therefore, inclusion of TSD and 3-D effects should not significantly alter the buckling response. The excellent agreement between the 3-D solution and the classical solution is considered verification of the buckling analysis. Agreement is equally good for all times greater than $t=0$.

Results and Discussion

A set of parametric studies was conducted to assess systematically the effects of laminate configuration, plate width-to-length ratio (b/a), plate length-to-thickness aspect ratio (a/h), and applied load ratio (N_y/N_x) on viscoelastic buckling behavior.

A set of three laminates possessing different anisotropy ratios was investigated using 3-D analysis for the case of a square plate loaded in uniaxial compression ($N_y=0$) with a/h held constant at 227.0. The results in Fig. 2 show the critical buckling load normalized by the buckling load at $t=0$ vs time for each laminate. Not only is the magnitude of the critical buckling load a function of laminate configuration, but also the viscoelastic behavior varies significantly. The $[0]_{24}$ laminate shows greater than twice the viscoelastic sensitivity of the quasiisotropic laminate. The reason for this becomes apparent when the results of the parametric study on biaxial loading effects are discussed.

Figure 3 shows normalized critical buckling load as a function of b/a for a $[0/\pm 45/90]_{3s}$ laminate subjected to uniaxial compression. Over the range investigated the isochronous curves show that critical buckling load is sensitive to b/a in the same manner as for elastic analysis. Comparison of the curves at $t=0$ and 1000 h reveal that viscoelastic effects are more severe at the lower ratios of b/a. A similar set of results is shown in Fig. 4 for a/h. Comparison of the isochronous buckling results revealed that the viscoelastic effects are stronger at lower values of a/h (for thicker laminates). In both of these cases, the viscoelastic effects are most pronounced for geometries which are most sensitive to transverse shear deformations.

Results from the study of load ratio effects in viscoelastic buckling response are shown in Fig. 5. The plots show the normalized buckling load as a function of time for values of N_y/N_x ranging from 0.0 to 1.0. Normalized results from classical analysis for all values of N_y/N_x superpose onto the $N_y/N_x=0$ curve. The normalized 3-D analysis results indicate a pronounced viscoelastic sensitivity which increases with increasing N_y/N_x. This increased viscoelastic sensitivity under conditions of biaxial stress is important, since fully constrained plates see biaxial stress states for all cases of mechanical, thermal, and hygroscopic loading. The more orthotropic the viscoelastic properties for a particular laminate, the greater the sensitivity, hence the reason for a $[0]_{24}$ laminate exhibiting greater viscoelastic sensitivity than a $[0/\pm 45/90]_{3s}$ laminate.

Conclusions

The viscoelastic buckling behavior of composite laminated plates has been investigated. The results from studies have shown that for a plate simply supported on all four boundaries, laminate configuration, plate geometry, and loading conditions all impart significant effects on the viscoelastic buckling response. The short time (<200 h) viscoelastic response results in the most significant decrease in buckling resistance, after which the long-term changes are very gradual. These results were obtained using linear viscoelasticity theory, which yields conservative results. More accurate results could be obtained using nonlinear viscoelastic theory, which would increase the time-dependent effects for some properties.

Implicit in these results is the concept of the differential viscoelastic sensitivity of laminate stiffness properties. Matrix-controlled properties, such as transverse shear modulus, exhibit stronger viscoelastic response than fiber-controlled properties. For this reason, classical analysis underestimates viscoelastic buckling behavior in cases where transverse shear and normal responses are involved. These observations suggest that it is important to include bending-extensional coupling, transverse shear deformation, and transverse normal deformation in viscoelastic buckling analyses of laminated plates. Omission of these effects causes misleading results which, according to the present study, can overpredict buckling loads by greater than 50% (see Fig. 5).

References

[1]Vinson, J. R. and Chou, T. W., *Composite Materials and Their Use in Structures*, John Wiley and Sons, Inc., New York, N. Y., 1975, pp. 201-309.

[2]Schapery, R. A., "Viscoelastic Behavior and Analysis of Composite Materials," *Composite Materials*, Vol. 2, G. P. Sendeckyj, editor, Academic Press, New York, N.Y., 1974, pp. 85-168.

[3]Halpin, J. C., "Introduction to Viscoelasticity," *Composite Materials Workshop*, G. P. Sendeckyj, editor, Technomic Publishing Co., Inc., Westport, Conn., 1968, pp. 87-151.

[4]Whitney, J. M., "The Effect of Transverse Shear Deformation on the Bending of Laminated Plates," *Journal of Composite Materials*, Vol. 3, July 1969, pp. 534-547.

[5]Wu, C. I. and Vinson, J. R., "Influence of Large Amplitudes, Transverse Shear Deformation and Rotary Inertia on Lateral Vibrations of Transversely Isotropic Plates," *Journal of Applied Mechanics*, July 1969, pp. 253-260.

[6]Sloan, J. G. and Vinson, J. R., "The Behavior of Rectangular Composite Materials Plates under Lateral and Hygrothermal Loads," University of Delaware, Newark, Del., AFSOR Scientific Report, AFOSR TR-78-1477, July 1978.

[7]Whitney, J. M., "The Effects of Boundary Conditions on the Response of Laminated Composites," *Journal of Composite Materials*, Vol. 4, April 1970, pp. 192-203.

[8]Flaggs, D. L. and Vinson, J. R., "Hygrothermal Effects on the Buckling and Laminated Composite Plates," *Fiber Science and Technology*, Vol. 11, 1978, pp. 353-366.

[9]Sims, D. F., "Viscoelastic Creep and Relaxation Behavior of Laminated Composite Plates," Ph.D. Dissertation, Southern Methodist University, Dallas, Texas, May 1972.

[10]Douglas, D. A. and Weitsman, Y., "Stresses Due to Environment Conditioning of Cross-Ply Graphite/Epoxy Laminates," *Proceedings of the Third International Conference on Composite Materials*, Paris, France, 1980.

[11]Pipes, R. B., Vinson, J. R., and Chou, T. W., "On Hygrothermal Response of Laminated Composite Systems," *Journal of Composite Materials*, Vol. 10, April 1976, p. 129.

[12]Tsai, S. W. and Hahn, H. T., *Introduction to Composite Materials*, Technomic Publishing Co., Inc., Westport, Conn., 1980.

[13]Wilson, D. W., "Viscoelastic Buckling Behavior of Laminated Plates," M.M.M.E. Thesis, University of Delaware, Newark, Del., June 1982.